The Plant Journal (2008) doi: 10.1111/j.1365-313X.2008.03445.x

A NIMA-related protein kinase suppresses ectopic outgrowth of epidermal cells through its kinase activity and the association with microtubules

Hiroyasu Motose[1,*], Rumi Tominaga[2], Takuji Wada[2], Munetaka Sugiyama[3] and Yuichiro Watanabe[1]

[1]*Department of Life Sciences, Graduate School of Arts & Sciences, The University of Tokyo, 3-8-1 Komaba, Meguro-ku, Tokyo 153-8902, Japan,*

[2]*Plant Science Center, RIKEN, 1-7-22 Suehiro-cho, Tsurumi-ku, Kanagawa 230-0045, Japan, and*

[3]*Botanical Gardens, Graduate School of Science, The University of Tokyo, 3-7-1 Hakusan, Bunkyo-ku, Tokyo 112-0001, Japan*

Received 11 September 2007; revised 29 January 2008; accepted 31 January 2008.
*For correspondence (fax +81 3 5454 6775; e-mail motose@bio.c.u-tokyo.ac.jp).

Summary

To study cellular morphogenesis genetically, we isolated loss-of-function mutants of *Arabidopsis thaliana*, designated *ibo1*. The *ibo1* mutations cause local outgrowth in the middle of epidermal cells of the hypocotyls and petioles, resulting in the formation of a protuberance. In Arabidopsis, the hypocotyl epidermis differentiates into two alternate cell files, the stoma cell file and the non-stoma cell file, by a mechanism involving *TRANSPARENT TESTA GLABRA1* (*TTG1*) and *GLABRA2* (*GL2*). The ectopic protuberances of the *ibo1* mutants were preferentially induced in the non-stoma cell files, which express *GL2*. TTG1-dependent epidermal patterning is required for protuberance formation in *ibo1*, suggesting that IBO1 functions downstream from epidermal cell specification. Pharmacological and genetic analyses demonstrated that ethylene promotes protuberance formation in *ibo1*, implying that IBO1 acts antagonistically to ethylene to suppress radial outgrowth. *IBO1* is identical to *NEK6*, which encodes a Never In Mitosis A (NIMA)-related protein kinase (Nek) with sequence similarity to Neks involved in microtubule organization in fungi, algae, and animals. The *ibo1-1* mutation, in which a conserved Glu residue in the activation loop is substituted by Arg, completely abolishes its kinase activity. The intracellular localization of GFP-tagged NEK6 showed that NEK6 mainly accumulates in cytoplasmic spots associated with cortical microtubules and with a putative component of the γ-tubulin complex. The localization of NEK6 is regulated by the C-terminal domain, which is truncated in the *ibo1-2* allele. These results suggest that the role of NEK6 in the control of cellular morphogenesis is dependent on its kinase action and association with the cortical microtubules.

Keywords: epidermis, ethylene, microtubule, NIMA-related kinase, protuberance.

Introduction

Epidermis, consisting of many specialized cells such as pavement cells, trichomes, guard cells, and root hair cells, provides a model system for studying cytodifferentiation in plants, which involves specification of cell fate and cellular morphogenesis (Hülskamp *et al.*, 1994). The specification processes of epidermal cells in shoots and roots are directed by a substantially common mechanism (reviewed by Hülskamp, 2004; Schiefelbein and Lee, 2006). The epidermal cell files in the root differentiate into either a trichoblast file that produces root hairs or an atrichoblast file that does not produce root hairs, and the hypocotyl epidermal cell files differentiate into a stoma-containing cell file or a non-stoma cell file (Berger *et al.*, 1998; Dolan *et al.*, 1994; Gendreau *et al.*, 1997; Hung *et al.*, 1998). The trichoblast and stoma cell files are positioned over the anticlinal cell wall between two cortex cell files, whereas the atrichoblast and non-stoma cell files are positioned outside the periclinal cell wall of one cortex cell file. A transcriptional complex containing a WD40-repeat protein TRANSPARENT TESTA GLABRA1 (TTG1; Walker *et al.*, 1999) promotes the expression of a homeodomain protein GLABRA2 (GL2; Rerie *et al.*, 1994) in a position-dependent manner, which prevents cell fate from

© 2008 The Authors
Journal compilation © 2008 Blackwell Publishing Ltd

being specified as root-hair cells or guard cells. *TTG1* and *GL2* are involved in trichome differentiation as well. Unlike the cases of root hair and guard cells, however, *GL2* positively regulates trichome differentiation.

Genetic analyses, biochemical studies, and live-cell imaging have revealed the central role of the organization of cortical microtubules in cellular morphogenesis as well as anisotropic growth (reviewed by Hamada, 2007; Hashimoto and Kato, 2005; Hussey *et al.*, 2002; Wasteneys and Yang, 2005). Microtubule-associated proteins (MAPs) bind to microtubules and participate in microtubule nucleation, stabilization, or destabilization (e.g. Smertenko *et al.*, 2000). Mutations in MAPs or tubulins have been known to cause various defects or abnormalities in anisotropic growth, cellular morphology, cell division, and microtubule organization (Abe *et al.*, 2004; Ambrose *et al.*, 2007; Buschmann *et al.*, 2004; Ishida *et al.*, 2007; Kawamura *et al.*, 2006; Kirik *et al.*, 2002; Nakajima *et al.*, 2004; Sedbrook *et al.*, 2004; Shoji *et al.*, 2004; Thitamadee *et al.*, 2002; Twell *et al.*, 2002; Whittington *et al.*, 2001). It has been also shown that the WAVE complex and the actin-related protein 2/3 (Arp2/3) complex, which enhance the initiation and branching of new actin microfilaments from pre-existing microfilaments, are essential for the morphogenesis of trichomes and the other epidermal cells (Basu *et al.*, 2004, 2005; Brembu *et al.*, 2004; Deeks *et al.*, 2004; El-Assal *et al.*, 2004a,b; Frank and Smith, 2002; Le *et al.*, 2003; Li *et al.*, 2003; Mathur *et al.*, 2003a,b; Uhrig *et al.*, 2007; reviewed by Smith, 2003). During pavement-cell morphogenesis in Arabidopsis, Rop-interactive CRIB motif-containing protein 4 (RIC4) locally activates a small G-protein ROP2, which enhances the assembly of cortical actin filaments and induces localized outgrowth (Fu *et al.*, 2002, 2005). Bundling of microtubules mediated by the other RIC family member, RIC1, antagonizes the RIC4–ROP2–actin pathway and inhibits localized outgrowth, resulting in interdigitating lobe-neck formation (Fu *et al.*, 2005).

Pharmacological and genetic analyses have indicated that protein phosphorylation is involved in the morphogenesis of epidermal cells (Baskin and Wilson, 1997; Camilleri *et al.*, 2002; Naoi and Hashimoto, 2004; Sakai *et al.*, 2008). Very recently, a Never In Mitosis A (NIMA)-related protein kinase (Nek), designated NEK6, has been identified as interacting with armadillo repeat-containing kinesin-related proteins (ARKs) (Sakai *et al.*, 2008). The *nek6* mutants exhibited pleiotropic phenotypes: side-by-side root-hair formation, abnormal protrusions in the hypocotyls and petioles, and a slightly leftward root growth (Sakai *et al.*, 2008). The *nek6-1* mutant also shows a reduction in trichome branching. From the observations that drugs interfering with microtubules partly phenocopied the *nek6* mutants and that *ark1* mutants accumulated extra microtubules in the endoplasm, NEK6 is inferred to act together with ARKs in the morphogenesis of epidermal cells via microtubule functions (Sakai *et al.*, 2008).

In the present study, we isolated a new class of loss-of-function mutants of Arabidopsis, designated *ibo1*, which exhibit abnormal protuberances on their epidermal cells. Positional cloning identified the gene responsible as *NEK6*. The *ibo1-1* mutation results in the complete loss of the kinase activity of NEK6, and green fluorescent protein (GFP)-NEK6 constructs labeled cytoplasmic spots associated with cortical microtubules. The localization pattern of GFP-NEK6 is interfered with by the *ibo1-2* mutation. Our findings suggest that NEK6 exerts a kinase function in a close relation with the cortical network of microtubules to suppress ectopic outgrowth and modulate anisotropic growth in epidermal cells.

Results

Phenotypic analysis of ibo1

The epidermal cells of the hypocotyls of wild-type Arabidopsis seedlings elongate simply and do not show outward growth. A series of novel mutants were originally isolated on the basis of protuberances on the surfaces of their hypocotyls, resulting from the unusual outward growth of the epidermal cells (Figure 1a). These mutants were referred to as '*ibo*', meaning 'small protuberances' in Japanese. Three recessive alleles of *ibo1* (*ibo1-1*, *ibo1-2*, and *ibo1-3*) were identified and characterized. The *ibo1-1* mutant was isolated from ethyl methane sulfonate (EMS)-mutagenized populations of the Wassilewskija accession (Ws). The *ibo1-2* and *ibo1-3* mutants were identified from EMS-mutagenized populations of the Columbia accession (Col). We also identified *ibo1-4* from T-DNA insertion populations (Alonso *et al.*, 2003), as described in a later section. Because all *ibo1* alleles were very similar in the protuberance phenotype, the *ibo1-1* mutant was mainly characterized in detail. In the *ibo1-1* seedlings, the epidermal protuberances were observed not only on the hypocotyls but also on the petioles of cotyledons and rosette leaves (Figure 1a,b). Each protuberance was a single-cell structure with a round tip, similar in appearance to a root hair (Figure 1c). Each of the protruding epidermal cells formed only one protuberance, in the middle of the cell (Figure 1c). The protuberances became visible 3–6 days after germination (Figure 1d), which corresponds to the linear growth phase of hypocotyls (Gendreau *et al.*, 1997).

In Arabidopsis hypocotyls, two kinds of epidermal cell files are arranged alternately into the non-stoma cell file and the stoma cell file (Berger *et al.*, 1998; Gendreau *et al.*, 1997; Hung *et al.*, 1998). We examined the relationship between these cell files and the protuberances in *ibo1*. Close observation of the hypocotyl surface of the *ibo1-1* mutant indicated that the protuberances are mostly restricted to the non-stoma cell files (Figure 1c), suggesting that the formation of protuberances is dependent on epidermal patterning.

© 2008 The Authors
Journal compilation © 2008 Blackwell Publishing Ltd,

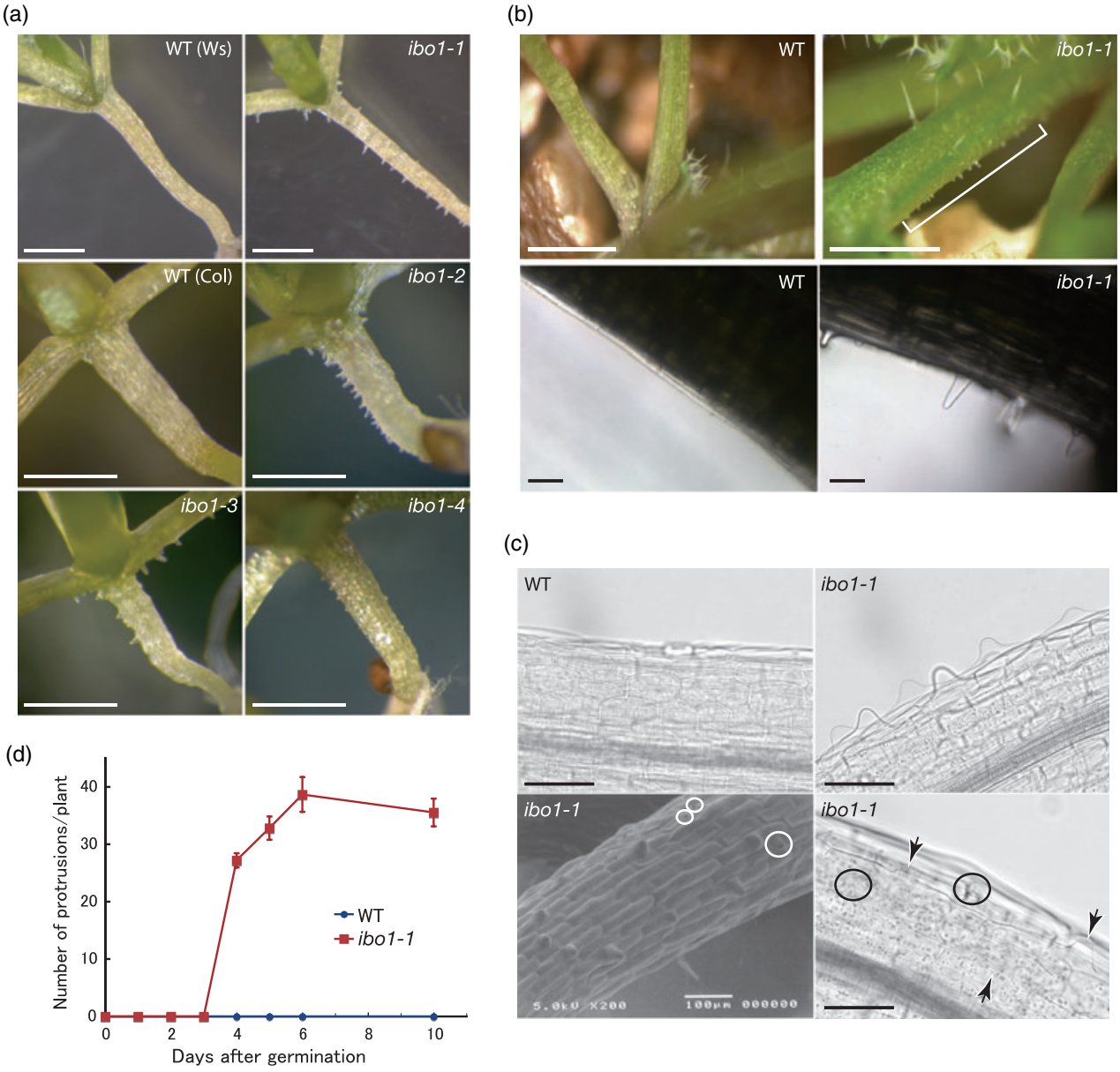

Figure 1. Phenotype of *ibo1*.
(a) Morphology of hypocotyls of 11-day-old seedlings of wild type and *ibo1*. Bars = 1 mm.
(b) Morphology of petioles of 21-day-old plants of wild type and *ibo1-1*: stereoscopic microscopy (upper panels, bars = 1 mm) or light microscopy (lower panels, bars = 100 μm). A bracket indicates protuberances in *ibo1-1*.
(c) Close observation of hypocotyl epidermis in wild type and *ibo1-1* by light microscopy (the upper panels and the lower right panel) and scanning electron microscopy (the lower left panel). Circles and arrows indicate stoma complexes and protuberances, respectively. Bars = 100 μm.
(d) Time course of protuberance formation. Symbols indicate averages of data from 25 seedlings of wild type (WT) and *ibo1-1*, and vertical lines represent SEs.

Next, we characterized the effects of the *ibo1* mutations on the trichomes and root hairs. Whereas the number of trichomes per leaf was not affected by any *ibo1* mutations (Figure S1), trichome branching was increased in *ibo1-2* (Table S1). With respect to root-hair density, there was no difference between the wild type and the *ibo1* mutants (Figure S2a,b). However, with regard to root-hair length, *ibo1-1* was slightly shorter and *ibo1-2* was rather longer than the wild type (Figure S2a,c).

Epidermal marker gene expression in ibo1

To characterize the *ibo1* phenotype in more detail, we analyzed the cell-specific expression of *GLABRA2* (*GL2*) and *EXPANSIN7* (*EXP7*). A glucuronidase (*GUS*) reporter gene was fused to the promoter region of *GL2* (P_{GL2}*::GUS*) or *EXP7* (P_{EXP7}*::GUS*), and these constructs were introduced into the wild type and *ibo1-1*. The GUS activity of the P_{GL2}*::GUS* lines was localized to the non-stoma cell files in

© 2008 The Authors
Journal compilation © 2008 Blackwell Publishing Ltd,

the hypocotyls (Figure 2a,c), the atrichoblast cell files in the roots (Figure 2e), and the trichomes in the leaves (Figure 2g). The GUS activity of the P_{EXP7}::GUS lines was specific to the root-hair cells (Figure 2i,k). These patterns of reporter gene expression are consistent with the results of previous studies (Masucci *et al.*, 1996; Ohashi *et al.*, 2003). The *ibo1* mutation did not affect the expression patterns of P_{GL2}::GUS or P_{EXP7}::GUS (Figure 2a–l). It is noteworthy that the epidermal cells undergoing protuberance formation in *ibo1-1* showed strong GUS activity in the P_{GL2}::GUS lines (Figure 2d) and no GUS activity in the P_{EXP7}::GUS lines (Figure 2j). These results indicate that the protuberances are induced in the non-stoma cell files expressing *GL2* and also suggest that the protuberance-forming cells are similar in gene expression to trichome cells rather than to root-hair cells.

Genetic relationship between epidermal regulators and IBO1

To test any possible genetic interactions of *IBO1* with the epidermal regulators *TTG1* and *CAPRICE* (*CPC*; Wada *et al.*, 1997), double mutant lines were generated and characterized for the hypocotyl phenotype (Figure 2m,n). *TTG1* is required for the promotion of *GL2* expression, which was prevented by *CPC* (Hülskamp, 2004). In the *ibo1-1 ttg1-1* double mutant, the protuberances were strongly suppressed, indicating that TTG1-dependent epidermal patterning is required for the formation of protuberances in *ibo1*. The *ibo1-1 cpc-1* double mutant formed protuberances like those of the *ibo1-1* single mutant. With respect to the trichome and root-hair phenotypes of *ttg1* and *cpc*, the *ibo1* mutations had neither an enhancing nor a suppressing effect. Like the *ttg1-1* single mutant, the *ibo1-1 ttg1-1* double mutant exhibited severe defects in trichome development and ectopic root-hair formation in the normally atrichoblast cell files. Like the *cpc-1* single mutant, root hairs were very few in the *ibo1-1 cpc-1* double mutant. The double-mutant analyses demonstrated that protuberance formation in *ibo1* involves *TTG1*, an important regulator required for trichome differentiation, but not CPC, a positive regulator of root-hair differentiation. This finding, together with the results for *GL2* expression, suggests that the *ibo1* protuberances might be trichome-like structures.

Ethylene promotes protuberance formation in ibo1

Ethylene is well known to have a function of controlling the radial growth of plant cells, and it has been shown that ethylene promotes root-hair formation and elongation in Arabidopsis (Masucci and Schiefelbein, 1994, 1996; Pitts *et al.*, 1998; Tanimoto *et al.*, 1995). Therefore, we examined the effects of the ethylene precursor, 1-amino-cyclopropane-1-carboxylic acid (ACC), and the ethylene biosynthesis inhibitor, aminoethoxyvinylglycine (AVG), on protuberance formation in *ibo1* (Figure 3a,b). When *ibo1-1* seedlings were grown on germination medium (GM) supplemented with ACC, the number of protuberances was markedly increased. In contrast, *ibo1-1* seedlings cultured on GM containing AVG had far fewer protuberances than the untreated *ibo1-1* seedlings. The reduction of protuberances by AVG was counteracted by the simultaneous addition of ACC, suggesting that AVG and ACC affect protuberance formation via changes in ethylene biosynthesis. No protuberances were induced in the epidermal cells of the wild-type hypocotyls by any treatment tested.

The effects of genetic modification of ethylene signaling on protuberance formation in *ibo1* were examined with *ibo1-1 ctr1-1* and *ibo1-1 ein2-1* double mutants. As shown in Figure 3(c,d), the *ibo1-1 ctr1-1* double mutant showed significantly increased protuberances on the hypocotyl epidermis, suggesting that the constitutive activation of ethylene signaling by the *ctr1-1* mutation enhanced protuberance formation in *ibo1-1*. In the *ibo1-1 ein2-1* double mutant, the number of protuberances was fewer than in the *ibo1-1* single mutant, suggesting a role for EIN2-dependent ethylene signaling in protuberance formation. Together, these results indicate the involvement of ethylene in protuberance formation in *ibo1*.

Enhanced elongation suppresses protuberance formation in ibo1

To test the possible relationship between *ibo1* protuberance formation and cell elongation, we examined the effects of dark-induced etiolation and gibberellic acid treatment (Figure 4). When hypocotyl elongation was stimulated by etiolation or gibberellic acid, the *ibo1-1* seedlings formed very few protuberances on their hypocotyls. This result indicates that the promotion of cell elongation antagonizes protuberance formation in *ibo1-1*.

IBO1 *encodes a NIMA-related protein kinase*

To determine the molecular basis of the *ibo1* phenotype, we identified the *IBO1* gene by map-based cloning (Figure 5a). The *IBO1* gene was localized between markers 43920 and 44400 on chromosome 3. By determining the nucleotide sequences of the candidate genes in this region, we found mutations in one gene, *At3g44200*, in all *ibo1* alleles (Figure 5b). Introduction of two genomic fragments (clones #1 and #2) encompassing *At3g44200* into *ibo1-2* recovered the normal phenotype (Figure 5c). A T-DNA insertion mutant of *IBO1* was identified in the collection of SALK T-DNA insertion lines and was designated *ibo1-4*. The *ibo1-4* mutant exhibited protuberances on its hypocotyls like the other *ibo1* mutants described above (Figure 1a). These results indicate that *At3g44200* is the *IBO1* gene. Because *At3g44200* was designated *AtNek6* or *NEK6* in previous reports (Cloutier

© 2008 The Authors
Journal compilation © 2008 Blackwell Publishing Ltd,

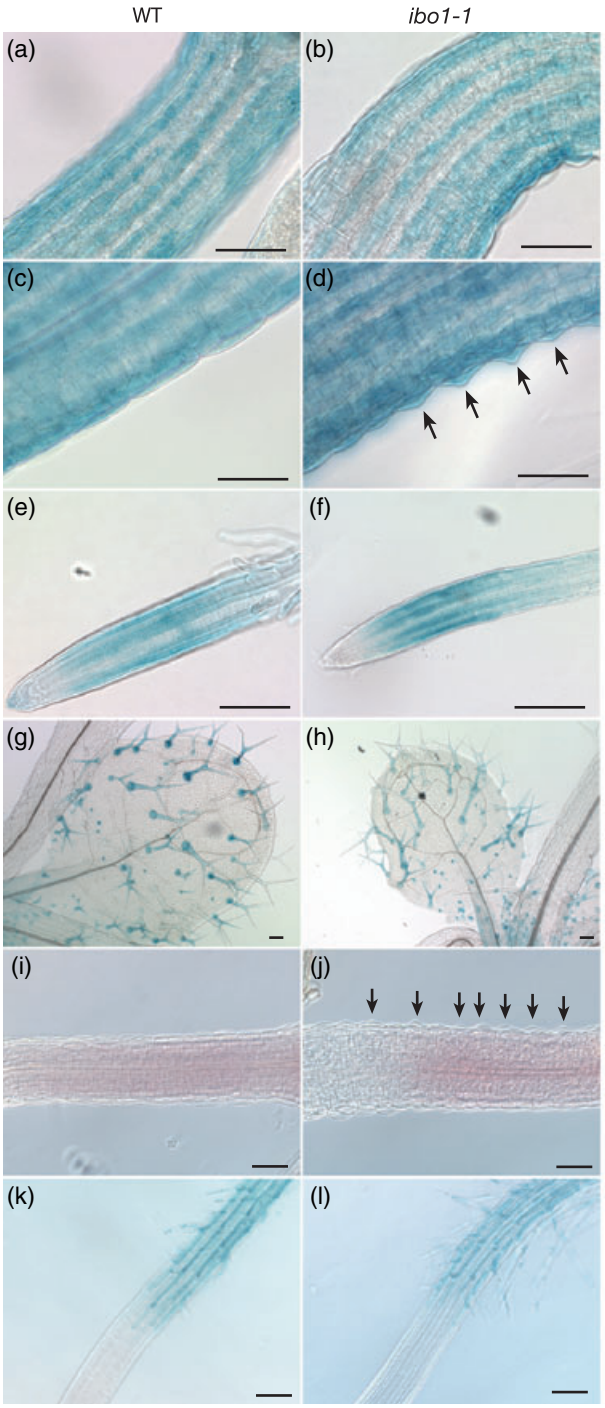

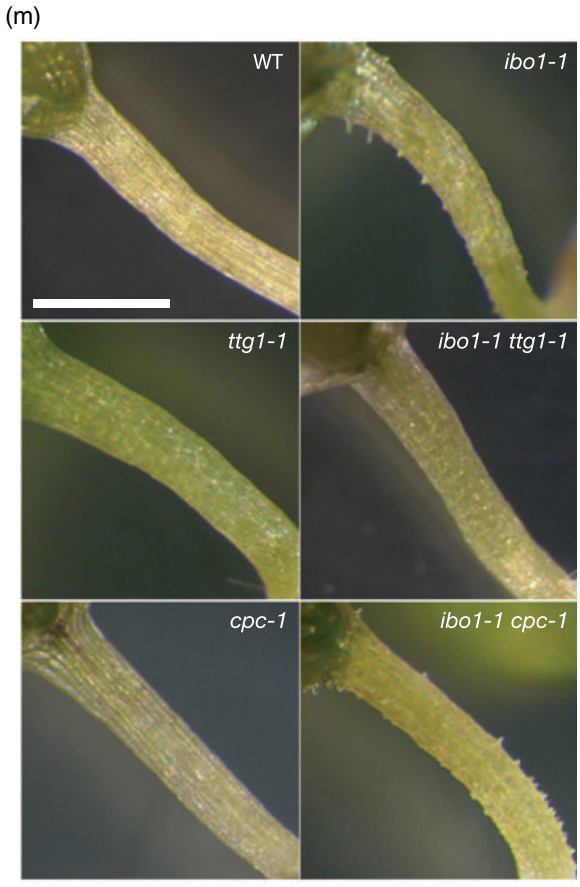

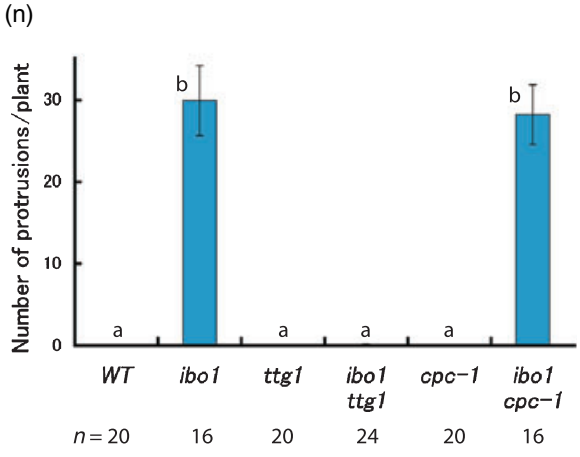

Figure 2. Relationship between epidermal cell patterning and protuberance formation in *ibo1*.
(a–h) GUS staining pattern of P_{GL2}*::GUS*. (a–d) Hypocotyls of 4-day-old seedlings of (a, c) wild type and (b, d) *ibo1-1*. (e, f) Roots and (g, h) leaves of 11-day-old seedlings of (e, g) wild type and (f, h) *ibo1-1*. Bars = 100 μm.
(i)–(l) GUS staining pattern of P_{EXP7}*::GUS*. (i, j) Hypocotyls and (k, l) roots of 4-day-old seedlings of (i, k) wild type and (j, l) *ibo1-1*. Bars = 100 μm.
(m) Morphology of hypocotyls of 11-day-old seedlings of wild type, *ibo1-1*, *ttg1-1*, *cpc-1*, *ibo1-1 ttg1-1*, and *ibo1-1 cpc-1*. Bar = 1 mm.
(n) Numbers of protuberances per hypocotyl were measured at 11 days after germination. Bars represent averages of data from 16 to 24 seedlings for each line. Vertical lines indicate SEs. Numbers of seedlings examined are indicated at the bottom. Values designated by the same letter are not significantly different at the $P = 0.01$ level in the Student's *t*-test.

© 2008 The Authors
Journal compilation © 2008 Blackwell Publishing Ltd,

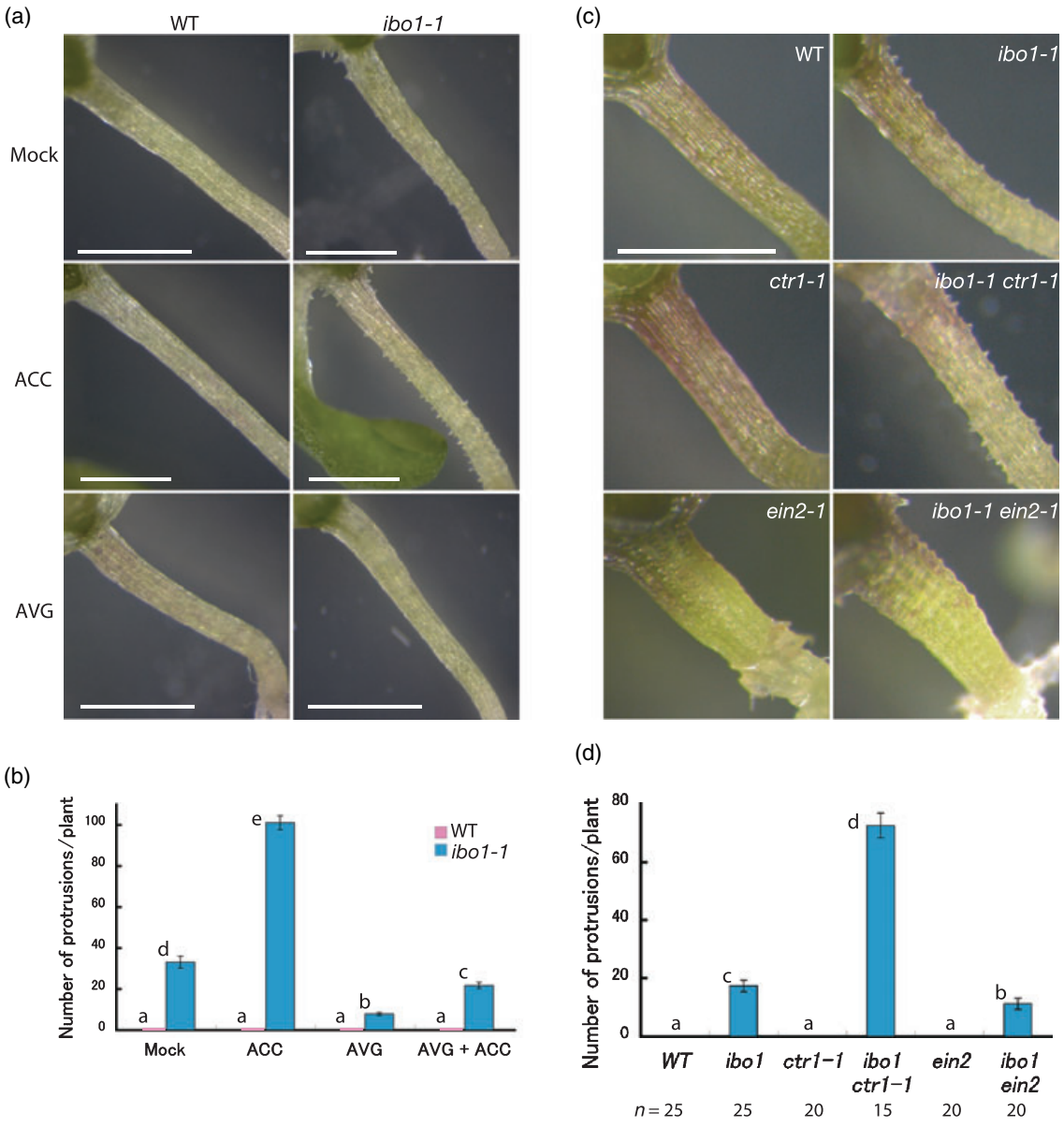

Figure 3. Ethylene promotes protuberance formation in *ibo1*.
(a, b) Wild type and *ibo1-1* were incubated for 11 days on GM without 1-amino-cyclopropane-1-carboxylic acid (ACC) and aminoethoxyvinylglycine (AVG) (Mock), with 100 μM ACC (ACC), with 5 μM AVG (AVG), or with 100 μM ACC and 5 μM AVG (AVG+ACC). (a) Morphology of hypocotyls of 11-day-old wild-type (Ws) and *ibo1-1* seedlings. Bars = 1 mm. (b) Numbers of protuberances per hypocotyl were calculated from 12 seedlings in each treatment at 11 days. Bars represent averages of data and vertical lines indicate SEs. Values designated by the same letter are not significantly different at the $P = 0.02$ level in the Student's *t*-test.
(c, d) Double mutant analysis. (c) Morphology of hypocotyl of 11-day-old wild type, *ibo1-1*, *ctr1-1*, *ein2-1*, *ibo1-1 ctr1-1*, and *ibo1-1 ein2-1*. Bar = 1 mm. (d) Numbers of protuberances per hypocotyl were calculated from 15 to 25 seedlings of each line at 11 days. Numbers of seedlings examined are indicated at the bottom. Bars represent averages of data and vertical lines indicate SEs. Values designated by the same letter are not significantly different at the $P = 0.04$ level in the Student's *t*-test.

et al., 2005; Sakai *et al.*, 2008), *IBO1* will be referred to as *NEK6* hereafter.

NEK6 is deduced to encode a protein of 956 amino acids, with a relative molecular mass of 106 388 and an isoelectric point of 6.76. Sequence analysis of NEK6 identified a Ser/Thr protein kinase domain at the N-terminus, which has significant homology to the kinase domains of the NIMA-related kinases of various organisms, including fungi, animals, and plants. In NEK6, the kinase domain is followed by a long tail containing three PEST degradation motifs and a coiled-coil domain near the C-terminus. The *ibo1-1* mutant allele has a G to A transition at nucleotide position 529, which causes an amino acid substitution of Glu177 with Arg in the activation loop of the kinase domain. The *ibo1-2* allele has a C to T

© 2008 The Authors
Journal compilation © 2008 Blackwell Publishing Ltd,

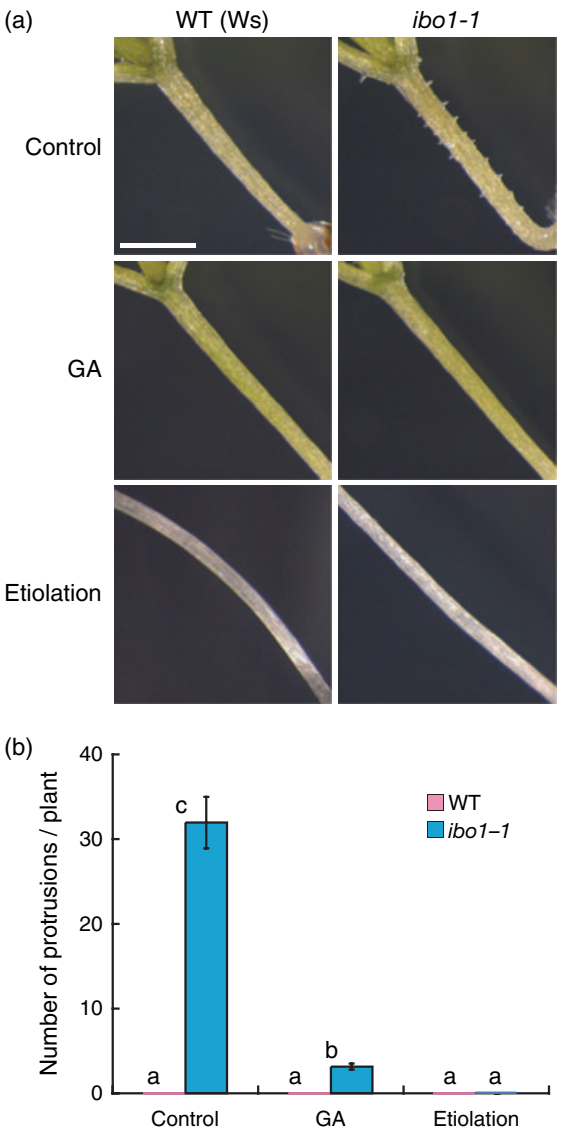

Figure 4. Enhanced elongation suppresses protuberance formation in *ibo1*.
(a, b) Wild type and *ibo1-1* were incubated for 11 days in continuous light without gibberellic acid (GA_3) (Control) or with 10 μM GA_3 (GA), or in the dark (Etiolation).
(a) Morphology of hypocotyls of 11-day-old wild type and *ibo1-1* seedlings. Bar = 1 mm.
(b) Numbers of protuberances per hypocotyl were calculated from 20 seedlings of each treatment at 11 days. Bars represent averages of data and vertical lines indicate SEs. Values designated by the same letter are not significantly different at the $P = 0.01$ level in the Student's *t*-test.

transition at nucleotide position 1978, which alters the Gln660 codon to a stop codon and might result in the production of a truncated NEK6 protein without the C-terminal half, which contains the coiled-coil domain. The *ibo1-3* allele has a C to T transition at nucleotide position 2746, which replaces Pro916 with Thr in the C-terminal region. Careful comparison with the amino acid sequences of plant Neks found a conserved sequence at the C-terminus following the coiled-coil domain (Figure 5b), which we designated the 'plant NEK C-terminal motif' (PNC motif). The Pro residue altered by the *ibo1*-3 mutation is highly conserved in this motif.

Reverse transcription (RT)-PCR analysis detected the *NEK6* transcripts in all the organs examined, especially in roots, inflorescence stems, and flowers (Figure 5d). The accumulation of the *NEK6* transcripts was not significantly altered in *ibo1-1* but was slightly reduced in *ibo1-2* and *ibo1-3* (Figure 5d).

Kinase activity of NEK6

To investigate the protein kinase activity of NEK6, a recombinant protein glutathione *S*-transferase (GST)-NEK6, in which full-length NEK6 was fused at its N-terminus to GST, was expressed in *Escherichia coli*, purified with glutathione beads, and assayed for *in vitro* kinase activity (Figure 6). After electrophoresis of GST-NEK6 that had been incubated with [γ-^{32}P]ATP, a radioactive band was detected at the position of GST-NEK6, indicating autophosphorylation activity of NEK6 (Figure 6a). When GST-NEK6 was incubated with myelin basic protein (MBP), an intense signal corresponding to the MBP band was detected, indicating transphosphorylation activity of NEK6 on MBP (Figure 6a). A requirement of NEK6 kinase activity for divalent cations was determined for both the autophosphorylation and the phosphorylation of MBP (Figure 6a). The addition of Mn^{2+} and Mg^{2+} to the reaction mixture produced strong and weak phosphorylation activities, respectively. No phosphorylation activity was detected with Ca^{2+} or in the absence of cations. The phosphorylation activity of GST-NEK6 incubated in buffer containing both Mn^{2+} and Mg^{2+} was slightly lower than that in buffer containing only Mn^{2+}. These results indicate that NEK6 requires Mn^{2+} or Mg^{2+} but not Ca^{2+}, and prefers Mn^{2+} to Mg^{2+}.

The *ibo1-1* allele has an Arg substitution at Glu177, which occurs at the C-terminal end of the activation loop and is conserved in various kinase families, including the Nek family. The autophosphorylation of the Ser/Thr residues in the activation loop of the Nek proteins is required for full kinase activity (Rellos *et al.*, 2007; Roig *et al.*, 2005). To examine whether the *ibo1-1* mutation results in either the loss or reduction of the kinase activity of NEK6, the *ibo1-1* mutation (E177R) was introduced into GST-NEK6. We also generated two kinase-dead negative controls (K37D and D133A) and three mutant proteins with single mutations at the putative phosphorylation sites of the activation loop (T157A, S166A, and T170A). The wild-type GST-NEK6 and mutated GST-NEK6 proteins were subjected to a kinase assay (Figure 6b). The *ibo1-1* mutation (E177R) and the kinase-dead mutations (K37D and D133A) resulted in a total loss of kinase activity. The T157A mutation reduced the kinase activity. The mutations S166A and T170A greatly

© 2008 The Authors
Journal compilation © 2008 Blackwell Publishing Ltd,

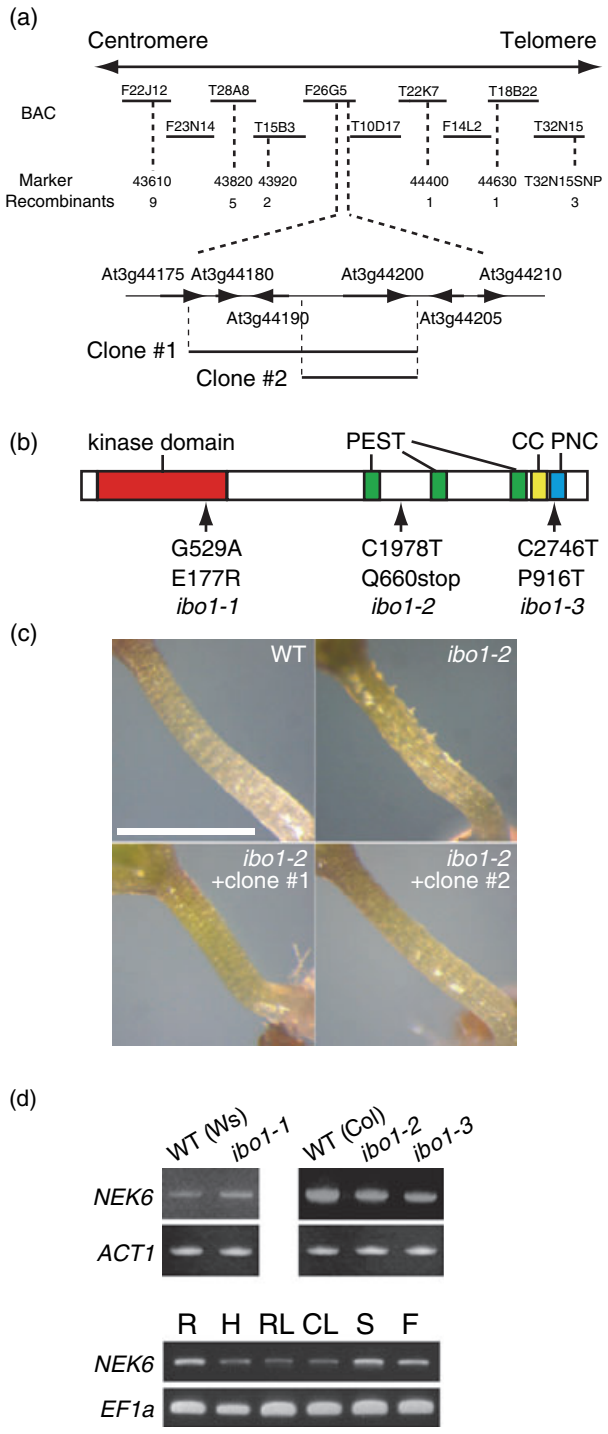

Figure 5. Positional cloning and expression analysis of *NEK6*.
(a) Chromosome mapping. BAC, markers, and recombinants are shown in schematic representation on chromosome 3. Clones #1 and #2 represent genomic clones used for complementation. Arrows represent positions and directions of genes.
(b) Schematic representation of NEK6. Kinase domain (red), PEST sequences (green, PEST), coiled-coil domain (yellow, CC), plant Nek C-terminal motif (blue, PNC) and mutation sites (arrow) are indicated.
(c) Complementation of the *ibo1* phenotype by the genomic clones. Morphology of hypocotyls of 7-day-old seedlings of wild type (Col), *ibo1-2*, and *ibo1-2* transformed with clone #1 (*ibo1-2* + clone #1) or with clone #2 (*ibo1-2* + clone #2). Bar = 1 mm.
(d) The RT-PCR analysis of *NEK6*. Upper panels: expression of *NEK6* in 11-day-old seedlings of wild type (Ws), *ibo1-1*, wild type (Col), *ibo1-2*, and *ibo1-3*. *ACT1* was used as a control. Lower panels: expression of *NEK6* in roots (R), hypocotyls (H), rosette leaves (RL), cauline leaves (CL), inflorescence stems (S), and flowers (F) of 1-month-old wild-type Col plants. *EF1a* was used as a control.

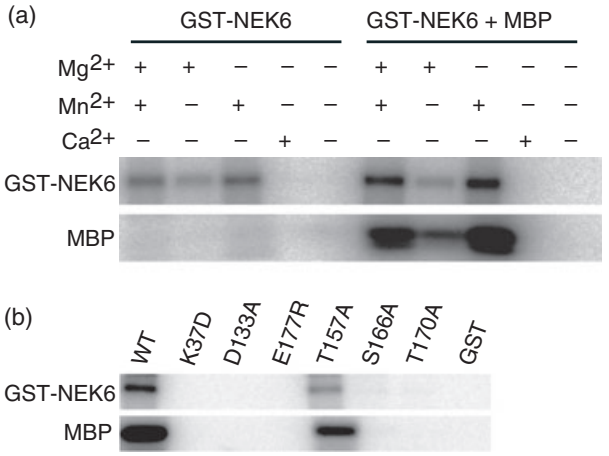

Figure 6. Kinase activity of NEK6.
(a) Purified GST-NEK6 was incubated in the kinase buffer containing 10 mM concentrations of cations with myelin basic protein (MBP) (GST-NEK6 + MBP) or without MBP (GST-NEK6). The plus and minus represent the presence and absence of cation(s) in the buffer, respectively.
(b) Effects of point mutations on the kinase activity of NEK6. The mutation indicated above each lane was introduced into GST-NEK6. Each purified protein was incubated in the buffer containing 10 mM Mn^{2+} with MBP.

reduced the phosphorylation activity to the basal level, suggesting that these Ser/Thr residues are essential for the activation of NEK6 by autophosphorylation.

Association of NEK6 with microtubules

To investigate the intracellular localization of NEK6, NEK6 fused at the N-terminus to GFP was transiently expressed in leaves of *Nicotiana benthamiana*. Strong fluorescence was observed in small dots aligned along the cortical filamentous structures (Figure 7a). Some of the strongly fluorescent dots were localized at the branching points of the filamentous structures. The GFP-NEK6 fluorescence pattern suggests that NEK6 is associated with cortical microtubules. To test this possibility, leaves were treated with the microtubule-stabilizing drug taxol, or the microtubule-depolymerizing drug oryzalin. Treatment with taxol intensified the fluorescent labeling of the filamentous structures (Figure 7a). In the presence of oryzalin, the filamentous structures disappeared, whereas the cortical fluorescent dots remained (Figure 7a). However, treatment with an actin microfilament-depolymerizing drug, latrunculin B, did not significantly affect the localization of GFP-NEK6 (Figure 7a).

© 2008 The Authors

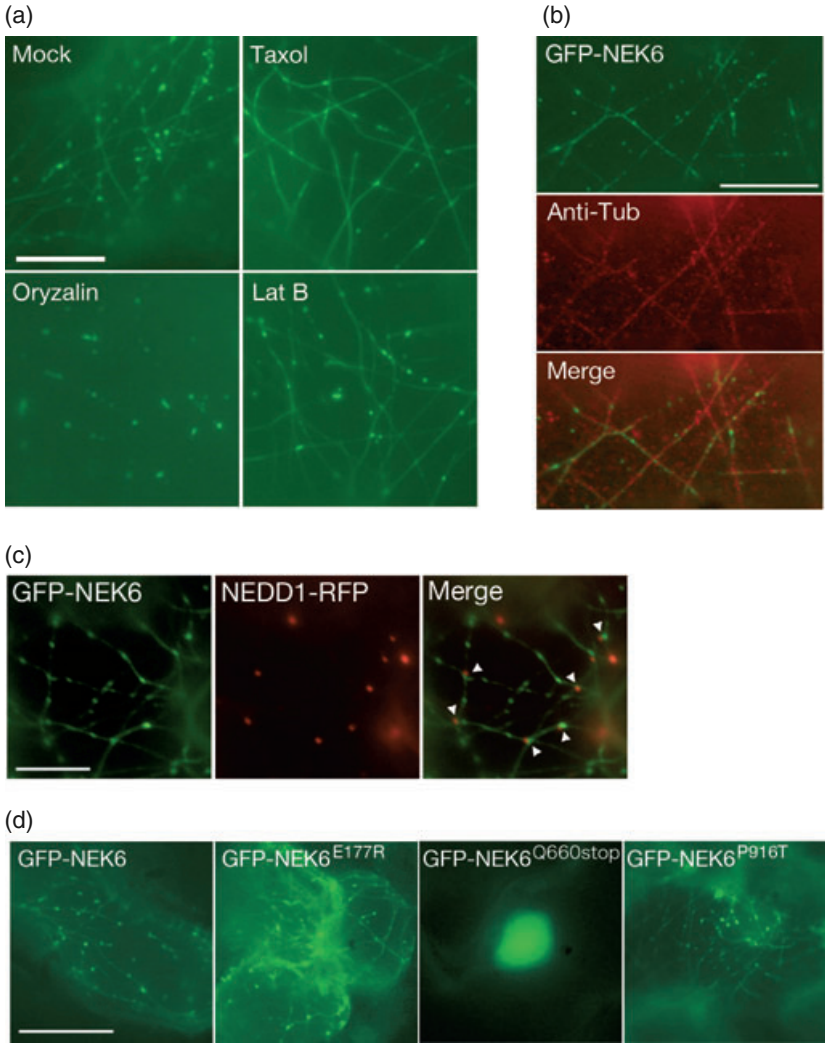

Figure 7. Subcellular localization of NEK6.
(a) Effects of inhibitors on subcellular localization of GFP-NEK6. GFP-NEK6 was transiently expressed in leaves of *Nicotiana benthamiana* by agroinfiltration. At 2 days after inoculation, leaf pieces were incubated without drug (Mock) or with 10 μM concentrations of taxol, oryzalin, or latrunculin B (Lat B) for 1 h and subjected to a fluorescence microscopy. Bar = 10 μm.
(b) Localization of GFP-NEK6 and microtubules. Microtubules in leaves of *N. benthamiana* expressing GFP-NEK6 were visualized with anti-tubulin antibody. Bar = 10 μm.
(c) Localization of GFP-NEK6 and NEDD1-mRFP. GFP-NEK6 and NEDD1-mRFP was transiently expressed in leaves of *N. benthamiana* and observed at 2 days after inoculation. Bar = 10 μm.
(d) Localization of mutant GFP-NEK6. Wild-type GFP-NEK6 and the *ibo1* mutant GFP-NEK6 were transiently expressed in leaves of *N. benthamiana* and analyzed at 2 days after inoculation. Bar = 20 μm.

When the cells expressing GFP-NEK6 were immunolabeled for microtubules, the fluorescent dots and filaments of GFP-NEK6 were observed along with the cortical microtubules (Figure 7b). All these results showed that NEK6 is localized in association with the cortical microtubules.

To further characterize the small dots labeled with GFP-NEK6, a putative ortholog of NEDD1, a component of the γ-tubulin complex (Haren *et al.*, 2006; Luders *et al.*, 2006), was co-expressed in a monomeric red fluorescent protein (mRFP)-fused form (NEDD1-mRFP) with GFP-NEK6 (Figure 7c). The GFP-NEK6 dots at the branching points of the microtubules were localized in close proximity to the dots labeled with NEDD1-mRFP, suggesting some relationships of NEK6 with the NEDD1-containing γ-tubulin complex.

We also analyzed the subcellular localization of the *ibo1* mutant NEK6 proteins (Figure 7d). GFP-NEK6^{E177R}, GFP-NEK6^{Q660stop}, and GFP-NEK6^{P916T} contain the *ibo1-1*, *ibo1-2*, and *ibo1-3* mutations, respectively. GFP-NEK6^{E177R} and GFP-NEK6^{P916T} labeled cytoplasmic spots associated with the cortical filaments, as did the wild-type GFP-NEK6, whereas GFP-NEK6^{Q660stop} localized preferentially to the nucleus (Figure 7d). These results imply that the C-terminal

© 2008 The Authors
Journal compilation © 2008 Blackwell Publishing Ltd,

region containing the coiled-coil domain (amino acids 660–956), which is truncated by the *ibo1-2* mutation, is required for the association of NEK6 with microtubules.

To evaluate the roles of NEK6 in the regulation of microtubules, the orientation of cortical microtubules in the hypocotyl epidermis was examined by confocal immunofluorescence microscopy (Figure S3). The majority of the cortical microtubules were arrayed transversely to the long axis of cells in the wild type. In *ibo1-1*, the orientation angles of microtubules centered around 90° but were slightly more deviated than the wild type. In statistical analysis using the Kolmogorov–Smirnov test, however, no significant difference was detected between the wild type and *ibo1-1*.

Discussion

Involvement of NEK6 in the morphogenesis of epidermal cells

In this paper we have described a new class of Arabidopsis mutants, *ibo1*, which have protuberances on the surfaces of their hypocotyls and petioles, arising from local outgrowth of epidermal cells. *IBO1* is identical to *NEK6* and encodes a Ser/Thr protein kinase that belongs to the Nek family. An *in vitro* kinase assay indicated that the *ibo1-1* mutation results in the total loss of NEK6 activity (Figure 6). These results strongly suggest that NEK6 functions as a suppressor of ectopic outgrowth in the epidermis through its kinase activity. Our results are consistent with the findings of Sakai *et al.* (2008) that T-DNA insertion mutants of *NEK6* and transgenic lines expressing the *NEK6* RNAi construct exhibited aberrant protuberances on their hypocotyls and petioles.

Although our knowledge of plant NEKs is quite limited and fragmentary, previous studies have identified the *NEK* gene family in plants and suggested their physiological roles in several aspects of development involving cell division (Cloutier *et al.*, 2005; Pnueli *et al.*, 2001; Vigneault *et al.*, 2007; Zhang *et al.*, 1996). Tomato (*Lycopersicon esculentum*) NEK (SPAK) interacts with SELF-PRUNING and a 14-3-3 protein and may regulate shoot development and flowering (Pnueli *et al.*, 2001). Poplar (*Populus tremula* × *alba*) *NEK* (*PNek1*) mRNA is expressed at the G_1/S transition and throughout the G_2 to M progression in synchronous cell culture (Cloutier *et al.*, 2005), and at sites of auxin synthesis *in planta* (Vigneault *et al.*, 2007). Phenotype analysis of the *PNek1* overexpressor in Arabidopsis (Cloutier *et al.*, 2005) and expression analysis of poplar and Arabidopsis *NEKs* (Vigneault *et al.*, 2007) suggest their involvement in organ and tissue development. Unlike these NEKs, NEK6 was implicated in the regulation of cell expansion and growth instead of cell division, since the *nek6* and *ibo1* mutants showed abnormalities only in cellular morphogenesis due to local outgrowth without detectable dysfunction of the meristems.

The *nek6* mutants exhibit not only abnormal protrusions on the hypocotyls and petioles but also various developmental defects in epidermal cells including side-by-side formation of root hairs and decrease in trichome branching (Sakai *et al.*, 2008). The morphological alterations in the root hairs and trichomes were also observed in the *ibo1* mutants (Figure 1 and Figures S1 and S2). In the trichome phenotype, however, there is a notable difference among mutants. Whereas trichome branching was decreased in *nek6-1*, it was increased in *ibo1-2*. This might reflect allele-specific dysfunctions of NEK6.

Because the *ibo1* and *nek6* mutants have no obvious defects in the elongation of cells and organs, the protuberance phenotype should not be attributed to a growth defect in the longitudinal direction. However, treatment with gibberellic acid or etiolation in the dark, which promotes hypocotyl elongation, suppressed protuberance formation in *ibo1* (Figure 4), suggesting an antagonistic relationship between longitudinal growth and protuberance outgrowth.

Molecular function of NEK6

Nek genes have been found in various eukaryotes, and their cognate proteins diverge in structure and possibly also in function (O'Connell *et al.*, 2003; Quarmby and Mahjoub, 2005). The NIMA kinase of *Aspergillus nidulans*, the first identified Nek, regulates the G_2/M transition and the progression of mitosis (Osmani *et al.*, 1988, 1991). Animal Nek2 and Nercc1 localize to the centrosomes, conspicuous microtubule organizing centers (MTOCs), and regulate centrosome separation (Rellos *et al.*, 2007; Roig *et al.*, 2005). Several other Nek proteins play important roles in the regulation of ciliary length and have been linked to polycystic kidney disease (reviewed by Quarmby and Mahjoub, 2005). Although these functions of Neks are physiologically diverse, they might all be related to the regulation of microtubule dynamics and MTOCs.

Several lines of evidence imply the involvement of NEK6 in the function of cortical microtubules. Arabidopsis seedlings treated with taxol or propyzamide exhibit a similar phenotype to that of the *nek6* mutants (Sakai *et al.*, 2008). NEK6 binds to kinesin-related proteins (ARKs), one of which (ARK1) might promote the destabilization of endoplasmic microtubules (Sakai *et al.*, 2008). In this study, we have demonstrated the microtubule-associated localization of GFP-NEK6 (Figure 7). GFP-NEK6 strongly labeled cortical dots along with microtubules. This pattern is reminiscent of the localization of several MAPs (Fu *et al.*, 2005; Kawamura *et al.*, 2006; Twell *et al.*, 2002; Wang *et al.*, 2007) and γ-tubulin (Murata *et al.*, 2005). Some of the cortical dots labeled with GFP-NEK6 appeared to localize at the branching points of microtubules, close to NEDD1, an ortholog of a component of the γ-tubulin complex (Figure 7). Although our preliminary data suggest that GFP-NEK6 is biologically

© 2008 The Authors
Journal compilation © 2008 Blackwell Publishing Ltd,

functional, the interpretation of the localization of GFP-NEK6 might be controversial because it is possible that constitutive expression of GFP-NEK6 masked the endogenous localization of NEK6.

Pioneering work using *Nitella* internodal cells (Wasteneys and Williamson, 1989a,b) indicated that the cortical microtubule array has a self-organizing property and new microtubules are formed along pre-existing microtubules, resulting in the branching of microtubules (Wasteneys, 2002). The microtubule-nucleating complex might be dissected from the minus ends, be moved along the existing microtubules by various kinesins (Liu and Lee, 2001), and nucleate additional microtubules (Wasteneys, 2002). Recently, Murata *et al.* (2005) demonstrated that the γ-tubulin complex is recruited onto pre-existing microtubules and that microtubule nucleation occurs on extant microtubules. Our results suggest that NEK6 associates with MTOCs at the branching points of microtubules. However, the immunocytological analysis of the microtubules could not detect any clear significant defect in the microtubule orientation in *ibo1-1*. This might be attributable to the mild and cell-type-specific phenotype of *ibo1*. A serial analysis of microtubule dynamics in living cells might be useful to detect microtubule abnormalities in the *ibo1* and *nek6* mutants.

Our results together with the findings of Sakai *et al.* (2008) implied that the function of NEK6 in preventing outgrowth of epidermal cells requires its association with cortical microtubules. In this regard, the *spr1* and *spr2* mutants are of special interest. These mutants exhibit ectopic root-hair-like protrusions on the upper hypocotyls when cultured in the dark for a long time at 4°C (Furutani *et al.*, 2000). *SPR1/SKU6* and *SPR2/TOR1* encode microtubule-associated proteins (Buschmann *et al.*, 2004; Nakajima *et al.*, 2004; Sedbrook *et al.*, 2004; Shoji *et al.*, 2004). This also suggests that a microtubule-dependent system participates in the suppression of ectopic outgrowth.

Although the present study did not address the regulatory mechanisms of NEK6, the results described here are suggestive for these problems. Kinase assay experiments showed a requirement for Mn^{2+} and Ser/Thr residues in the activation loop for the kinase activity of NEK6. The mislocalization of GFP-NEK6^{Q660stop} into the nucleus suggests that the C-terminal region containing the coiled-coil domain is required for the association of NEK6 with microtubules. This result may be related to the previous observation that the C-terminal tail is required for the proper localization of PNek1 (Cloutier *et al.*, 2005). In addition, the *ibo1-3* mutation suggests a significance of the PNC motif for the biological activity of NEK6, the molecular function of which remains to be determined.

An important clue for possible factors regulating NEK6 is the observation that the kinesin-related proteins, ARKs, interact with the C-terminal region of NEK6 (Sakai *et al.*, 2008). This result reminds us of the activation of the tobacco MAP kinase kinase kinase, NPK1, by the NACK1 and NACK2 kinesin-like proteins (Nishihama *et al.*, 2002). In this MAP kinase cascade (NACK-PQR pathway), the MAP kinase NRK1 phosphorylates a microtubule-associated protein, NtMAP65-1, downregulates its activity, and controls phragmoplast formation (Sasabe *et al.*, 2006). The analogy suggests that NEK6 is activated or recruited to microtubules by its interaction with ARKs. The functional relationship between NEK6 and ARKs is under investigation.

NEK6 and specification of cell fate

The formation of protuberances in *ibo1* is related to the patterning of epidermal cells. The hypocotyl epidermis in Arabidopsis differentiates into two alternating cell files, the non-stoma cell file and the stoma cell file, dependent on the TTG1/GL2 pathway (Berger *et al.*, 1998; Gendreau *et al.*, 1997; Hung *et al.*, 1998). TTG1 is required for the promotion of *GL2* expression in the non-stoma cell files, and GL2 suppresses the differentiation of stoma cell files. The *ttg1-1* mutation causes the loss of *GL2* expression and ectopic stoma formation in the non-stoma cell files (Berger *et al.*, 1998; Hung *et al.*, 1998). Protuberance formation in the non-stoma cell files (Figures 1 and 2) and the suppression of protuberances by *ttg1-1* (Figure 3) indicate that the TTG1-dependent differentiation of non-stoma cell files is required for protuberance formation in *ibo1*. The epidermal cells in the non-stoma cell files are larger than those in stoma cell files and have a convex morphology, suggesting that these cells may have a tendency to expand radially and are competent to form protuberances, which is suppressed by NEK6 activity in the wild type (summarized in Figure S4).

There have been several papers reporting ectopic outgrowth of epidermal cells caused by the loss-of-function mutations or genetic modifications of epidermal regulators (Hu and Ma, 2006; Kirik *et al.*, 2004; Larkin *et al.*, 1994; Ohashi *et al.*, 2003). The *etc1-1 try-82 cpc-1* triple mutant develops abundant trichomes on its hypocotyls (Kirik *et al.*, 2004), suggesting that ETC1, TRY, and CPC suppress the differentiation of the hypocotyl epidermal cells into trichomes. The overexpression of both *GL1* and maize *R* genes also caused the development of ectopic trichomes on hypocotyls (Larkin *et al.*, 1994), demonstrating that the overexpression of *GL1* and *R* could overwhelm and/or bypass the inhibitory effects of ETC1, TRY, and CPC on trichome specification. The overexpression of *MINI ZINC FINGER1* or *VP16-GL2ΔN* induced ectopic root-hair development on hypocotyls (Hu and Ma, 2006; Ohashi *et al.*, 2003). These studies indicate that the hypocotyl epidermis is competent to form trichomes and root hairs, and that this competence is sequestered by a transcriptional network involving both positive and negative regulators.

It should be noted that the *nek6* mutants and *NEK6* RNAi transgenic lines show side-by-side root-hair formation

© 2008 The Authors

(Sakai *et al.*, 2008). It is not clear whether this phenotype is due to the disorganization of the cell files or ectopic root-hair formation in the atrichoblast files. If the latter is true, the suppressive action of NEK6 on ectopic outgrowth might be common to both hypocotyls and roots, because the *ibo1* protuberances were formed in the non-stoma cell files, which correspond to the atrichoblast files in roots.

NEK6 and ethylene

In the Arabidopsis root, ethylene treatment causes ectopic root-hair formation in the positions where atrichoblast cells are normally located, suggesting that ethylene is a positive signal controlling the position-dependent differentiation of root hairs (Tanimoto *et al.*, 1995). Detailed analysis indicated that ethylene triggers root-hair morphogenesis downstream from the patterning process regulated by the TTG1/GL2 pathway (Masucci and Schiefelbein, 1996). In this study, we have demonstrated that ethylene promotes protuberance formation in *ibo1*. Furthermore, the *ein2* mutation reduced the *ibo1* protuberances and the *ctr1* mutation increased the protuberances in *ibo1*. Hence, endogenous ethylene signaling is involved in the ectopic outgrowth of epidermal cells in *ibo1*. Unlike the case of root hairs, ethylene did not alter the cell file positions of protuberance formation in *ibo1*. Ethylene enhanced protuberance formation in *ibo1* in the non-stoma cell files but not in the stoma cell files (data not shown), suggesting that ethylene affects cell morphogenesis rather than cell specification. One possible hypothesis is that NEK6 suppresses the promotion by ethylene of the ectopic outgrowth of epidermal cells (Figure S4).

Interestingly, Kazama *et al.* (2004) found that the transient exposure of etiolated cucumber seedlings to ethylene induced snorkel-like multicellular protuberances in the less differentiated regions of the hypocotyls, while in the differentiating regions of the hypocotyls, ethylene treatment modified stomatogenesis and trichome formation. These results indicate that ectopic outgrowth in the hypocotyl epidermis can be caused by ethylene alone under some situations. How epidermal cells are released by ethylene from the regulation by NEK6 in such cases is an intriguing problem.

Experimental procedures

Plant materials and growth conditions

To isolate the *ibo1* mutants, the wild-type Ws and Col seeds were treated with 0.1% solution of EMS for 16 h at room temperature. Approximately 10 000 M_2 seedlings were screened for protuberances on the hypocotyl epidermis. The P_{GL2}*::GUS* line and *cpc-1* are described in Wada *et al.* (2002, 1997), respectively. The P_{EXP7}*::GUS* line (Ohashi *et al.*, 2003) was kindly provided by Dr Takashi Aoyama (Kyoto University, Japan). The *ttg1-1*, *ctr1-1*, and *ein2-1* seeds were provided from the Arabidopsis Biological Resource Center (ABRC). The seeds and information about *ibo1-4* (SALK_152782) were obtained from the SIGnAL website (http://signal.salk.edu) and ABRC. For growth of seedlings, surface-sterilized seeds were plated on germination medium [GM, half-strength Murashige and Skoog salts containing Gamborg B5 vitamins and 10 g l^{-1} sucrose buffered with 0.5 g l^{-1} (*N*-morpholino)ethanesulfonic acid to pH 5.7 and solidified with 0.25% gellan gum]. After 2 days at 4°C, plates were incubated at 22°C in continuous light.

Chromosome mapping

Mapping was carried out by DNA analysis with simple sequence length polymorphism (Bell and Ecker, 1994) and cleaved amplified polymorphic sequence markers (Konieczny and Ausubel, 1993).

Complementation

Genomic clones #1 and #2 were isolated from the transformation-competent genomic library (Ohtani and Sugiyama, 2005) and used for complementation analysis. Arabidopsis plants were transformed by the floral dip method (Clough and Bent, 1998).

RT-PCR

Total RNA was extracted as described previously (Ozeki *et al.*, 1990). After treatment with RNase-free DNase I (Invitrogen, http://www.invitrogen.com/), first strand cDNA was synthesized with Superscript III (Invitrogen) according to the manufacturer's instructions and was used as a template for PCR with gene-specific primer sets (Table S2) for 30 cycles (*IBO1*), 25 cycles (*ACT1*), 25 cycles (*EF1a*).

GUS staining

Samples of GUS lines were stained as described (Wada *et al.*, 2002).

GFP-IBO1

The DNA fragment containing the full-length open reading frame (ORF) for *IBO1* was cloned into a Gateway® (Invitrogen) binary vector of pGWB6 that provides a N-terminal GFP fusion protein driven by the CaMV35S promoter (Nakagawa *et al.*, 2007a). The NEDD1 ORF fragment was cloned into a Gateway® binary vector that provides a C-terminal mRFP fusion protein driven by the CaMV35S promoter (Nakagawa *et al.*, 2007b). Transient expression of GFP-IBO1 and NEDD1-mRFP in leaves of *N. benthamiana* was performed by agroinfiltration (Yang *et al.*, 2000; Yuasa *et al.*, 2005).

Immunofluorescence

Indirect immunofluorescence staining was performed to visualize microtubules according to Wasteneys *et al.* (1997) and Sugimoto *et al.* (2000). Rat monoclonal anti-α-tubulin antibody YL1/2 (Abcam, http://www.abcam.com/) was used as a first antibody at the dilution of 1/100. Alexa 568 anti-rat-IgG antibody (Invitrogen) or fluorescein isothiocyanate (FITC)-conjugated anti-rat-IgG antibody (Sigma-Aldrich, http://www.sigmaaldrich.com/) was used as a secondary antibody at a dilution of 1/250. Quantitative analysis of microtubule orientation was done as described by Sugimoto *et al.* (2003).

© 2008 The Authors
Journal compilation © 2008 Blackwell Publishing Ltd,

Microscopy

Arabidopsis plants were observed using a stereoscopic microscope MZ12 (Leica Microsystems, http://www.leica-microsystems.com/) equipped with DFC480 CCD camera. A DM5000B (Leica) equipped with DFC480 was used for the light microscopy and fluorescence microscopy. An LSM510 (Zeiss, http://www.zeiss.com/) was used for the confocal laser scanning microscopy. Scanning electron microscopy was performed according to Tsukaya *et al.* (1993) with a JSM-5200LV (JEOL, http://www.jeol.com/).

Kinase assay in vitro

The cDNA encoding the full-length *IBO1* was cloned into the GST fusion vector pGEX4T-2 (GE Healthcare, http://www.gehealthcare.com/). The point mutations were introduced by the KOD-plus mutagenesis kit (TOYOBO, http://www.toyobo.co.jp/e/). One microgram of the GST-tagged recombinant proteins was incubated with or without 1 μg MBP in 20 μl of kinase buffer containing 10 μCi [γ-^{32}P]ATP at 24°C for 30 min. Reaction products were separated by SDS-PAGE and detected by autoradiography.

The detailed experimental procedure is available in Appendix S1.

Acknowledgements

We thank Takashi Aoyama (Kyoto University) for the P_{EXP7}::GUS seeds; Tsuyoshi Nakagawa (Shimane University) for pGWBs; ABRC for Arabidopsis seeds; and SIGnAL for T-DNA lines; Toshio Sano and Seiichiro Hasezawa (The University of Tokyo) and Tatsuya Sakai (RIKEN) for valuable advice and discussion. This work was supported by Grants-in-Aids from the Ministry of Education, Sports, Culture, Science and Technology of Japan (no. 18770028), the Asahi Glass Foundation, and the Sumitomo Foundation to HM.

Supplementary Material

The following supplementary material is available for this article online:

Figure S1. Effect of *ibo1* mutations on the density of trichomes.

Figure S2. Effects of *ibo1* mutations on the density and length of root hairs.

Figure S3. Cortical microtubules in the wild type and *ibo1-1*.

Figure S4. Hypothetical scheme for the NEK6 function in cellular morphogenesis.

Table S1. Effect of *ibo1* mutations on trichome branching.

Table S2. Primers used in this study.

Appendix S1. Detailed experimental procedures.

This material is available as part of the online article from http://www.blackwell-synergy.com.

Please note: Blackwell Publishing are not responsible for the content or functionality of any supplementary materials supplied by the authors. Any queries (other than missing material) should be directed to the corresponding author for the article.

References

Abe, T., Thitamadee, S. and Hashimoto, T. (2004) Microtubule defects and cell morphogenesis in the *lefty1lefty2* tubulin mutant of *Arabidopsis thaliana*. *Plant Cell Physiol.* **45**, 211–220.

Alonso, J.M., Stepanova, A.N., Leisse, T.J. *et al.* (2003) Genome-wide Insertional mutagenesis of *Arabidopsis thaliana*. *Science*, **301**, 653–657.

Ambrose, J.C., Shoji, T., Kotzer, A.M., Pighin, J.A. and Wasteneys, G.O. (2007) The *Arabidopsis CLASP* gene encodes a microtubule-associated protein involved in cell expansion and growth. *Plant Cell*, **19**, 2763–2775.

Baskin, T.I. and Wilson, J.E. (1997) Inhibitors of protein kinases and phosphatases alter root morphology and disorganize cortical microtubules. *Plant Physiol.* **113**, 493–502.

Basu, D., El-Assal, S.E., Le, J., Mallery, E.L. and Szymanski, D.B. (2004) Interchangeable functions of Arabidopsis PIROGI and the human WAVE complex subunit SRA-1 during leaf epidermal morphogenesis. *Development*, **131**, 4345–4355.

Basu, D., Le, J., El-Assal, S.E., Huang, S., Zhang, C., Mallery, E.L., Koliantz, G., Staiger, C.J. and Szymanski, D.B. (2005) DISTORTED3/SCAR2 is a putative Arabidopsis WAVE complex subunit that activates the Arp2/3 complex and is required for epidermal morphogenesis. *Plant Cell*, **17**, 502–524.

Bell, C.J. and Ecker, J.R. (1994) Assignment of 30 microsatellite loci to the linkage map of Arabidopsis. *Genomics*, **19**, 137–144.

Berger, F., Linstead, P., Dolan, L. and Haseloff, J. (1998) Stomata patterning on the hypocotyls of *Arabidopsis thaliana* is controlled by genes involved in the control of root epidermis patterning. *Dev. Biol.* **194**, 226–234.

Brembu, T., Winge, P., Seem, M. and Bones, A.M. (2004) *NAPP* and *PIRP* encode subunits of a putative Wave regulatory protein complex involved in plant cell morphogenesis. *Plant Cell*, **16**, 2335–2349.

Buschmann, H., Fabri, C.O., Hauptmann, M., Hutzler, P., Laux, T., Lloyd, C.W. and Schaffner, A.R. (2004) Helical growth of the Arabidopsis mutant *tortifolia1* reveals a plant-specific microtubule-associated protein. *Curr. Biol.* **14**, 1515–1521.

Camilleri, C., Azimzadeh, J., Pastuglia, M., Bellini, C., Grandjean, O. and Bouchez, D. (2002) The Arabidopsis *TONNEAU2* gene encodes a putative novel protein phosphatase 2A regulatory subunit essential for the control of the cortical cytoskeleton. *Plant Cell*, **14**, 833–845.

Clough, S.J. and Bent, A.F. (1998) Floral dip: a simplified method for *Agrobacterium*-mediated transformation of *Arabidopsis thaliana*. *Plant J.* **16**, 735–743.

Cloutier, M., Vigneault, F., Lachance, D. and Séguin, A. (2005) Characterization of a popular NIMA-related kinase PNek1 and its potential role in meristematic activity. *FEBS Lett.* **579**, 4659–4665.

Deeks, M.J., Kaloriti, D., Davies, B., Malho, R. and Hussey, P.J. (2004) Arabidopsis NAP1 is essential for Arp2/3-dependent trichome morphogenesis. *Curr. Biol.* **14**, 1410–1414.

Dolan, L., Duckett, C.M., Grierson, C., Linstead, P., Schneider, K., Lawson, E., Dean, C., Poethig, S. and Roberts, K. (1994) Clonal relationships and cell patterning in the root epidermis of Arabidopsis. *Development*, **120**, 2465–2474.

El-Assal, S.E., Le, J., Basu, D., Mallery, E.L. and Szymanski, D.B. (2004a) *DISTORTED2* encodes an ARPC2 subunit of the putative Arabidopsis ARP2/3 complex. *Plant J.* **38**, 526–538.

El-Assal, S.E., Le, J., Basu, D., Mallery, E.L. and Szymanski, D.B. (2004b) Arabidopsis *GNARLED* encodes a NAP125 homologue that positively regulates ARP2/3. *Curr. Biol.* **14**, 1405–1409.

Frank, M.J. and Smith, L.G. (2002) A small, novel protein highly conserved in plants and animals promotes the polarized growth and division of maize leaf epidermal cells. *Curr. Biol.* **12**, 849–853.

Fu, Y., Li, H. and Yang, Z.B. (2002) The ROP2 GTPase controls the formation of cortical fine F-actin and the early phase of directional cell expansion during Arabidopsis organogenesis. *Plant Cell*, **14**, 777–794.

© 2008 The Authors

Fu, Y., Gu, Y., Zheng, Z.L., Wasteneys, G. and Yang, Z.B. (2005) Arabidopsis interdigitating cell growth requires two antagonistic pathways with opposing action on cell morphogenesis. *Cell*, **120**, 687–700.

Furutani, I., Watanabe, Y., Prieto, R., Masukawa, M., Suzuki, K., Naoi, K., Thitamadee, S., Shikanai, T. and Hashimoto, T. (2000) The *SPIRAL* genes are required for directional control of cell elongation in *Arabidopsis thaliana*. *Development*, **127**, 4443–4453.

Gendreau, E., Traas, J., Desnos, T., Grandjean, O., Caboche, M. and Höfte, H. (1997) Cellular basis of hypocotyl growth in *Arabidopsis thaliana*. *Plant Physiol.* **114**, 295–305.

Hamada, T. (2007) Microtubule-associated proteins in higher plants. *J. Plant Res.* **120**, 79–98.

Haren, L., Remy, M.H., Bazin, I., Callebaut, I., Wright, M. and Merdes, A. (2006) NEDD1-dependent recruitment of the gamma-tubulin ring complex to the centrosome is necessary for centriole duplication and spindle assembly. *J. Cell Biol.* **172**, 505–515.

Hashimoto, T. and Kato, T. (2005) Cortical control of plant microtubules. *Curr. Opin. Plant Biol.* **8**, 1–7.

Hu, W. and Ma, H. (2006) Characterization of a novel putative zinc finger gene *MIF1*: involvement in multiple hormonal regulation of Arabidopsis development. *Plant J.* **45**, 399–422.

Hülskamp, M. (2004) Plant trichomes: a model for cell differentiation. *Nat. Rev. Mol. Cell Biol.* **5**, 471–480.

Hülskamp, M., Misera, S. and Jürgens, G. (1994) Genetic dissection of trichome cell development in Arabidopsis. *Cell*, **76**, 555–566.

Hung, C.Y., Lin, Y., Zhang, M., Pollock, S., Marks, M.D. and Schiefelbein, J. (1998) A common position-dependent mechanism controls cell-type patterning and GLABRA2 regulation in the root and hypocotyl epidermis of Arabidopsis. *Plant Physiol.* **117**, 73–84.

Hussey, P.J., Hawkins, T.J., Igarashi, H., Kaloriti, D. and Smertenko, A. (2002) The plant cytoskeleton: recent advances in the study of the plant microtubule-associated proteins MAP-65, MAP-190 and the Xenopus MAP215-like protein, MOR1. *Plant Mol. Biol.* **50**, 915–924.

Ishida, T., Kaneko, Y., Iwano, M. and Hashimoto, T. (2007) Helical microtubule arrays in a collection of twisting tubulin mutants of *Arabidopsis thaliana*. *Proc. Natl Acad. Sci. USA*, **104**, 8544–8549.

Kawamura, E., Himmelspach, R., Rashbrooke, M.C., Whittington, A.T., Gale, K.R., Collings, D.A. and Wasteneys, G.O. (2006) MICROTUBULE ORGANIZATION1 regulates structure and function of microtubule arrays during mitosis and cytokinesis in the Arabidopsis root. *Plant Physiol.* **140**, 102–114.

Kazama, H., Dan, H., Imaseki, H. and Wasteneys, G.O. (2004) Transient exposure to ethylene sitimulates cell division and alters the fate and polarity of hypocotyl epidermal cells. *Plant Physiol.* **134**, 1614–1623.

Kirik, V., Grini, P.E., Mathur, J., Klinkhammer, I., Adler, K., Bechtold, N., Herzog, M., Bonneville, J.M. and Hülskamp, M. (2002) The Arabidopsis tubulin-folding cofactor A gene is involved in the control of the alpha/beta-tubulin monomer balance. *Plant Cell*, **14**, 2265–2276.

Kirik, V., Simon, M., Hülskamp, M. and Schiefelbein, J. (2004) The *ENHANCER OF TRY AND CPC1* gene acts redundantly with *TRIPTYCHON* and *CAPRICE* in trichome and root hair cell patterning in Arabidopsis. *Dev. Biol.* **268**, 506–513.

Konieczny, A. and Ausubel, F.M. (1993) A procedure for mapping *Arabidopsis* mutations using co-dominant ecotype-specific PCR-based markers. *Plant J.* **4**, 403–410.

Larkin, J.C., Oppenheimer, D.G., Lloyd, A.M., Paparozzi, E.T. and Marks, M.D. (1994) Roles of the *GLABROUS1* and *TRANSPARENT TESTA GLABRA* genes in Arabidopsis trichome development. *Plant Cell*, **6**, 1065–1076.

Le, J., El-Assal, S.E., Basu, D., Saad, M.E. and Szymanski, D.B. (2003) Requirements for Arabidopsis ATARP2 and ATARP3 during epidermal development. *Curr. Biol.* **13**, 1341–1347.

Li, S., Blanchoin, L., Yang, Z. and Lord, E.M. (2003) The putative Arabidopsis Arp2/3 complex controls leaf cell morphogenesis. *Plant Physiol.* **132**, 2034–2044.

Liu, B. and Lee, Y.R.J. (2001) Kinesin-related proteins in plant cytokinesis. *J. Plant Growth Regul.* **20**, 141–150.

Luders, J., Patel, U.K. and Stearns, T. (2006) GCP-WD is a gamma-tubulin targeting factor required for centrosomal and chromatin-mediated microtubule nucleation. *Nat. Cell Biol.* **8**, 137–147.

Masucci, J.D. and Schiefelbein, J.W. (1994) The *rhd6* mutation of *Arabidopsis thaliana* alters root-hair initiation through an auxin-associated and ethylene-associated process. *Plant Physiol.* **106**, 1335–1346.

Masucci, J.D. and Schiefelbein, J.W. (1996) Hormones act downstream of *TTG* and *GL2* to promote root hair outgrowth during epidermis development in the Arabidopsis root. *Plant Cell*, **8**, 1505–1517.

Masucci, J.D., Rerie, W.G., Foreman, D.R., Zhang, M., Galway, M.E., Marks, M.D. and Schiefelbein, J.W. (1996) The homeobox gene *GLABRA 2* is required for position-dependent cell differentiation in the root epidermis of *Arabidopsis thaliana*. *Development*, **122**, 1253–1260.

Mathur, J., Mathur, N., Kernebeck, B. and Hülskamp, M. (2003a) Mutations in actin-related proteins 2 and 3 affect cell shape development in Arabidopsis. *Plant Cell*, **15**, 1632–1645.

Mathur, J., Mathur, N., Kirik, V., Kernebeck, B., Srinivas, B.P. and Hülskamp, M. (2003b) Arabidopsis *CROOKED* encodes for the smallest subunit of the ARP2/3 complex and controls cell shape by region specific fine F-actin formation. *Development*, **130**, 3137–3146.

Murata, T., Sonobe, S., Baskin, T.I., Hyodo, S., Hasezawa, S., Nagata, T., Horio, T. and Hasebe, M. (2005) Microtubule-dependent microtubule nucleation based on recruitment of gamma-tubulin in higher plants. *Nat. Cell Biol.* **7**, 961–968.

Nakagawa, T., Kurose, T., Hino, T., Tanaka, K., Kawamukai, M., Niwa, Y., Toyooka, K., Matsuoka, K., Jinbo, T. and Kimura, T. (2007a) Development of series of gateway binary vectors, pGWBs, for realizing efficient construction of fusion genes for plant transformation. *J. Biosci. Bioeng.* **104**, 34–41.

Nakagawa, T., Suzuki, T., Murata, S. *et al.* (2007b) Improved gateway binary vectors: high-performance vectors for creation of fusion constructs in transgenic analysis of plants. *Biosci. Biotechnol. Biochem.* **71**, 2095–2100.

Nakajima, K., Furutani, I., Tachimoto, H., Matsubara, H. and Hashimoto, T. (2004) *SPIRAL1* encodes a plant-specific microtubule-localized protein required for directional control of rapidly expanding Arabidopsis cells. *Plant Cell*, **16**, 1178–1190.

Naoi, K. and Hashimoto, T. (2004) A semidominant mutation in an Arabidopsis mitogen-activated protein kinase phosphatase-like gene compromises cortical microtubule organization. *Plant Cell*, **16**, 1841–1853.

Nishihama, R., Soyano, T., Ishikawa, M. *et al.* (2002) Expansion of the cell plate in plant cytokinesis requires a kinesin-like protein/MAPKKK complex. *Cell*, **109**, 87–99.

O'Connell, M.J., Krien, M.J.E. and Hunter, T. (2003) Never say never. The NIMA-related protein kinases in mitotic control. *Trends Cell Biol.* **13**, 221–228.

© 2008 The Authors
Journal compilation © 2008 Blackwell Publishing Ltd,

Ohashi, Y., Oka, A., Rodrigues-Pousada, R., Possenti, M., Ruberti, I., Morelli, G. and Aoyama, T. (2003) Modulation of phospholipids signaling by GLABRA2 in root-hair pattern formation. *Science*, **300**, 1427–1430.

Ohtani, M. and Sugiyama, M. (2005) Involvement of SRD2-mediated activation of snRNA transcription in the control of cell proliferation competence in Arabidopsis. *Plant J.* **43**, 479–490.

Osmani, S.A., Pu, R.T. and Morris, N.R. (1988) Mitotic induction and maintenance by overexpression of a G2-specific gene that encodes a potential protein kinase. *Cell*, **53**, 237–244.

Osmani, A.H., O'Donnell, K., Pu, R.T. and Osmani, S.A. (1991) Activation of the NIMA protein kinase plays a unique role during mitosis that cannot be bypassed by absence of the BimE checkpoint. *EMBO J.* **10**, 2669–2679.

Ozeki, Y., Matsui, K., Sakuta, M., Matsuoka, M., Ohashi, Y., Kano-Murakami, Y., Yamamoto, N. and Tanaka, Y. (1990) Differential regulation of phenylalanine ammonia-lyase genes during anthocyanin synthesis and by transfer effect in carrot suspension cultures. *Physiol. Plant.* **80**, 379–387.

Pitts, R.J., Cernac, A. and Estelle, M. (1998) Auxin and ethylene promote root hair elongation in *Arabidopsis*. *Plant J.* **16**, 553–560.

Pnueli, L., Gutfinger, T., Hareven, D., Ben-Naim, O., Ron, N., Adir, N. and Lifschitz, E. (2001) Tomato SP-interacting proteins define a conserved signaling system that regulates shoot architecture and flowering. *Plant Cell*, **13**, 2687–2702.

Quarmby, L.M. and Mahjoub, M.R. (2005) Caught Nek-ing: cilia and centrioles. *J. Cell Sci.* **118**, 5161–5169.

Rellos, P., Ivins, F., Baxter, J.E. *et al.* (2007) Structure and regulation of the human Nek2 centrosomal kinase. *J. Biol. Chem.* **282**, 6833–6842.

Rerie, W.G., Feldmann, K.A. and Marks, M.D. (1994) The *GLABRA2* gene encodes a homeo domain protein required for normal trichome development in Arabidopsis. *Genes Dev.* **8**, 1388–1399.

Roig, J., Groen, A., Caldwell, J. and Avruch, J. (2005) Active Nercc1 protein kinase concentrates at centrosomes early in mitosis and is necessary for proper spindle assembly. *Mol. Biol. Cell*, **16**, 4827–4840.

Sakai, T., van der Honing, H., Nishioka, M. *et al.* (2008) Armadillo repeat-containing kinesins and a NIMA-related kinase are required for epidermal-cell morphogenesis in Arabidopsis. *Plant J.* **53**, 157–171.

Sasabe, M., Soyano, T., Takahashi, Y., Sonobe, S., Igarashi, H., Itoh, T.J., Hidaka, M. and Machida, Y. (2006) Phosphorylation of NtMAP65-1 by a MAP kinase down-regulates its activity of microtubule bundling and stimulates progression of cytokinesis of tobacco cells. *Genes Dev.* **20**, 1004–1014.

Schiefelbein, J. and Lee, M.M. (2006) A novel regulatory circuit specifies cell fate in the Arabidopsis root epidermis. *Physiol. Plant.* **126**, 503–510.

Sedbrook, J.C., Ehrhardt, D.W., Fisher, S.E., Scheible, W.R. and Somerville, C.R. (2004) The Arabidopsis *SKU6/SPIRAL1* gene encodes a plus end-localized microtubule-interacting protein involved in directional cell expansion. *Plant Cell*, **16**, 1506–1520.

Shoji, T., Narita, N.N., Hayashi, K., Asada, J., Hamada, T., Sonobe, S., Nakajima, K. and Hashimoto, T. (2004) Plant-specific microtubule-associated protein SPIRAL2 is required for anisotropic growth in Arabidopsis. *Plant Physiol.* **136**, 3933–3944.

Smertenko, A., Saleh, N., Igarashi, H., Mori, H., Hauser-Hahn, I., Jiang, C.J., Sonobe, S., Lloyd, C.W. and Hussey, P.J. (2000) A new class of microtubule-associated proteins in plants. *Nat. Cell Biol.* **2**, 750–753.

Smith, L.G. (2003) Cytoskeletal control of plant cell shape: getting the fine points. *Curr. Opin. Plant Biol.* **6**, 63–73.

Sugimoto, K., Himmelspach, R., Williamson, R.E. and Wasteneys, G.O. (2003) Mutation or drug-dependent microtubule disruption causes radial swelling without altering parallel cellulose microfibril deposition in Arabidopsis root cells. *Plant Cell*, **15**, 1414–1429.

Sugimoto, K., Williamson, R.E. and Wasteneys, G.O. (2000) New techniques enable comparative analysis of microtubule orientation, wall texture, and growth rate in intact roots of Arabidopsis. *Plant Physiol.* **124**, 1493–1506.

Tanimoto, M., Roberts, K. and Dolan, L. (1995) Ethylene is a positive regulator of root hair development in *Arabidopsis thaliana*. *Plant J.* **8**, 943–948.

Thitamadee, S., Tuchihara, K. and Hashimoto, T. (2002) Microtubule basis for left-handed helical growth in Arabidopsis. *Nature*, **417**, 193–196.

Tsukaya, H., Naito, S., Rédei, G.P. and Komeda, Y. (1993) A new class of mutations in *Arabidopsis thaliana*, *acaulis1*, affecting the development of both inflorescences and leaves. *Development*, **118**, 751–764.

Twell, D., Park, S.K., Hawkins, T.J., Schubert, D., Schmidt, R., Smertenko, A. and Hussey, P.J. (2002) MOR1/GEM1 has an essential role in the plant-specific cytokinetic phragmoplast. *Nat. Cell Biol.* **4**, 711–714.

Uhrig, J.F., Mutondo, M., Zimmermann, I., Deeks, M.J., Machesky, L.M., Thomas, P., Uhrig, S., Rambke, C., Hussey, P.J. and Hülskamp, M. (2007) The role of Arabidopsis *SCAR* genes in ARP2-ARP3-dependent cell morphogenesis. *Development*, **134**, 967–977.

Vigneault, F., Lachance, D., Cloutier, M., Pelletier, G., Levasseur, C. and Séguin, A. (2007) Members of the plant NIMA-related kinases are involved in organ development and vascularization in popular, Arabidopsis, and rice. *Plant J.* **51**, 575–588.

Wada, T., Tachibana, T., Shimura, Y. and Okada, K. (1997) Epidermal cell differentiation in Arabidopsis determined by a *Myb* homolog, *CPC*. *Science*, **277**, 1113–1116.

Wada, T., Kurata, T., Tominaga, R., Koshino-Kimura, Y., Tachibana, T., Goto, K., Marks, M.D., Shimura, Y. and Okada, K. (2002) Role of a positive regulator of root hair development, CAPRICE, in Arabidopsis root epidermal cell differentiation. *Development*, **129**, 5409–5419.

Walker, A.R., Davison, P.A., Bolognesi-Winfield, A.C., James, C.M., Srinivasan, N., Blundell, T.L., Esch, J.J., Marks, M.D. and Gray, J.C. (1999) The *TRANSPARENT TESTA GLABRA1* locus, which regulates trichome differentiation and anthocyanin biosynthesis in Arabidopsis, encodes a WD40 repeat protein. *Plant Cell*, **11**, 1337–1349.

Wang, X., Zhu, L., Liu, B., Wang, C., Jin, L., Zhao, Q. and Yuana, M. (2007) *Arabidopsis* MICROTUBULE-ASSOCIATED PROTEIN18 functions in directional cell growth by destabilizing cortical microtubules. *Plant Cell*, **19**, 877–889.

Wasteneys, G.O. (2002) Microtubule organization in the green kingdom: chaos or self-order? *J. Cell Sci.* **115**, 1345–1354.

Wasteneys, G.O. and Williamson, R.E. (1989a) Reassembly of microtubules in *Nitella tasmanica* – assembly of cortical microtubules in branching clusters and its relevance to steady-state microtubule assembly. *J. Cell Sci.* **93**, 705–714.

Wasteneys, G.O. and Williamson, R.E. (1989b) Reassembly of microtubules in *Nitella tasmanica* – quantitative analysis of assembly and orientation. *Eur. J. Cell Biol.* **50**, 76–83.

Wasteneys, G.O. and Yang, Z. (2005) New views on the plant cytoskeleton. *Plant Physiol.* **136**, 3884–3891.

Wasteneys, G.O., Willingale-Theune, J. and Menzel, D. (1997) Freeze shattering: a simple and effective method for permeabilizing higher plant cell walls. *J. Microsc.* **188**, 51–61.

© 2008 The Authors
Journal compilation © 2008 Blackwell Publishing Ltd,

Whittington, A.T., Vugrek, O., Wei, K.J., Hasenbein, N.G., Sugimoto, K., Rashbrooke, M.C. and Wasteneys, G.O. (2001) MOR1 is essential for organizing cortical microtubules in plants. *Nature*, **411**, 610–613.

Yang, Y., Li, R. and Qi, M. (2000) *In vivo* analysis of plant promoters and transcription factors by agroinfiltration of tobacco leaves. *Plant J.* **22**, 543–551.

Yuasa, T., Sugiki, M. and Watanabe, Y. (2005) Activation of SIPK in response to UV-C irradiation: utility of a glutathione-S transferase-tagged plant MAP kinase by transient expression with agroinfiltration. *Plant Biotechnol.* **22**, 7–12.

Zhang, H., Scofield, G., Fobert, P. and Doonan, J.H. (1996) A nimA-like protein kinase transcript is highly expressed in meristems of *Antirrhinum majus*. *J. Microsc.* **181**, 186–194.

© 2008 The Authors
Journal compilation © 2008 Blackwell Publishing Ltd,